Saudi Journal of Biological Sciences 30 (2023) 103551

HOSTED BY

Contents lists available at ScienceDirect

Saudi Journal of Biological Sciences

journal homepage: www.sciencedirect.com

Original article

Apoptotic and antiproliferative effects of silk protein sericin conjugated-$AgNO_3$ nanoparticles in human breast cancer cells

Samaira Mumtaz [a], Shaukat Ali [a,*], Asim Pervaiz [b], Muhammad Zahid Qureshi [c], Kinzah Kanwal [b], Talha Saleem [b,d]

[a] Medical Toxicology and Entomology Laboratory, Department of Zoology, Government College University, Kechary Road Lahore, 54000 Lahore, Pakistan
[b] Institute of Biomedical and Allied Health Sciences, Khayaban-e-Jamia Punjab, Lahore-54600, University of Health Sciences Lahore, Pakistan
[c] Deanship of Educational Services, Department of Biochemistry, Qassim University, Buraydah, Al Qassim, Buraidah 51452, Saudi Arabia
[d] Department of Allied Health Sciences, Superior University, Lahore, Pakistan

ARTICLE INFO

Article history:
Received 28 September 2022
Revised 26 November 2022
Accepted 20 December 2022
Available online 26 December 2022

Keywords:
Sericin
Sericin-$AgNO_3$ NPs
Anti-proliferation
Apoptosis
Breast cancer
Cell cycle arrest GADD family

ABSTRACT

Bombyx mori silk sericin is a globular-like protein that is used as an antioxidant, antibacterial, and anti-tumor agent. In this current research, we isolated sericin by degumming process and formation of sericin-$AgNO_3$ NPs confirmed by UV–vis spectra, SEM, EDX, FTIR, and XRD patterns. The sericin and sericin-$AgNO_3$ NPs mediated changes in human breast cancer cells were determined. The antiproliferative activity of sericin-$AgNO_3$ NPs was analyzed by MTT dye reduction assay. Alterations at molecular levels were investigated by qRT-PCR, while apoptotic effects were studied by nuclear DNA staining. After 72 h treatment, sericin and sericin-$AgNO_3$ NPs showed significant antiproliferative effects in MDA-MB-231 (26 %) and MCF-7 (41 %) cells. Expression modification showed prominent stimulation of cell cycle arrest and stress related genes such as cyclin-dependent kinase inhibitors (CDKN1A, CDKN1B), and GADD family genes. RT-PCR results of the GADD family include GADD45A, B, G, 34, 153 and cyclin-dependent kinase inhibitors (CDKN1A, 1B) showed pronounced induction of 3.1 to 19.8-folds in MCF-7 cell line while induction in MDA-MB-231 cell line was 2.5 to 34.3-folds. Nuclear DAPI staining showed significant induction of apoptosis and nuclear fragmentation in MDA-MB-231 cells at a concentration of 1 mg/mL for both sericin and sericin-$AgNO_3$ NPs. Meanwhile, in case of MCF-7 cells, after treatment with sericin and sericin-$AgNO_3$ NPs (1 mg/mL), the cells changed into a round shape and lost their original spindle outlook in dose-dependent manners. We concluded that sericin-$AgNO_3$ NPs have significant antiproliferative, apoptosis, and genetic profiling effects in both breast cancer cell lines at the highest concentration.

1. Introduction

Worldwide, cancer is the foremost source of human being fatality and a chief community fitness apprehension. Generally, during various years, it can be defined as any part of the body having unrestrained expansion and proliferation of the cells occurring due to genetic alterations and harmful environmental factors. In the case of cancer, during the transformation process, important genes like tumor-suppressor and oncogene deregulate and this imbalance leads to lethal cellular changes (Casais-Molina et al., 2018). Breast cancers are widespread and destructive tumor types that affect the female population in the entire world (Han et al., 2018). Carcinoma of the breast is the second foremost of death due to cancer and the most frequent malignancy in women. It is a tumor of lobules supplying milk ducts, the inner lining of milk ducts, and breast tissues. The rate of the existence of breast tumors in developed and developing countries with an estimated 5 years is 80 % and 40 % respectively (Akram et al., 2017).

Bombyx mori silk cocoon is a natural source of silk sericin (SS) a globular-like protein composed mainly of fibroin protein (70–80 %) with sericin (20–30 %). In a silk cocoon, three silk sericin layers

* Corresponding author at: Medical Toxicology and Entomology Laboratory, Department of Zoology, Government College University, Kechary Road 1, Lahore, 54000 Lahore, Pakistan.
E-mail addresses: samaira.mumtaz@gcu.edu.pk (S. Mumtaz), dr.shaukatali@gcu.edu.pk (S. Ali), drasimpervaiz@uhs.edu.pk (A. Pervaiz), M.Qureshi@qu.edu.sa (M.Z. Qureshi), kinzah.kanwal480@uhs.edu.pk (K. Kanwal), talha.saleem@superior.edu.pk (T. Saleem).
Peer review under responsibility of King Saud University.

Production and hosting by Elsevier

https://doi.org/10.1016/j.sjbs.2022.103551
1319-562X/

including the outer layer hold 15 % sericin, the middle layer grip 10.5 %, and the inner layer compose 4.5 % with sericin surrounding the silk fibroin layer (Saha et al., 2019). Silk sericin synthesized by the labial gland of *B. mori* has a molecular weight of about 200 kDa due presence of polar amino acids that made it a hydrophilic-based glycoprotein. Mainly, it is composed of eighteen various kinds of amino acids but the largest part prevalent include glycine, serine, threonine, aspartic acid, tyrosine, and glutamic acid (Mody et al., 2009). Due to the highly enriched contents of carotenoids and flavonoids, it is responsible for anti-oxidant and anti-tyrosine actions. SS contains 6 % hydrogen, 16.5 % nitrogen, 31 % oxygen, and 46.5 % carbon which give its organic composition description (Mody et al., 2009). Sericin is used against various biological properties including anti-oxidant, moisture-absorbing capabilities, UV resistance, antibacterial, as well as antitumor actions. It can also be used for natural or synthetic fibers of textile industries as a finishing agent in addition to a biomedical polymeric product being as a skincare mediator in cosmetic industries (Joseph and Raj, 2012). For tumor therapy, the therapeutic index of chemotherapy agents has been significantly enhanced by the coming out of nanoparticle-based drug delivery approaches. However, nanoparticles (NPs) tend to be highly unstable and agglomerate when they come up to reach a fluid material (Hu et al., 2018).

Silver nanoparticles (AgNPs) are extensively applied in different areas of disciplines for the production of different biomedical yields to prevent various types of infectious diseases such as antibacterial, anti-inflammatory, antiviral, and anticancer therapies. Due to anti-oxidant and cytotoxicity properties, silver nanoparticles (AgNPs) mediated cytotoxicity via excess construction of ROS and induce disproportionate apoptosis in various cancerous and non-cancerous cells related to lung ovarian, and breast cancer (Bin-Jumah, et al., 2020). Silver nanoparticles also caused mitochondrial dysfunction leading to chromosomal aberrations and sets off DNA damage by releasing the free silver ions and ROS. Overcoming the problem of silver nanoparticles surface modification occurring with any dispersion agent may be a good sort. The dispersion stabilizers are highly hydrophilic polymers as well as polysaccharides would consist of their functionality, like drug-delivery approaches and cancer cures. In this study, silkworm (*Bombyx mori*) protein sericin is used as a hydrophilic polymeric stabilizer conjugated with AgNPs due to its good biodegradable and biocompatible properties. (Lv et al., 2018). The purpose of the conducted research was to elucidate the breast cancer potential of silkworm protein sericin and sericin-$AgNO_3$ NPs against two human breast cancer cell lines i.e., MCF-7 and MDA-MB-231.

2. Materials and methods

2.1. Ethics approval

The research study was ethically approved with reference No. GCU-IIB-1064 from Government College University, Lahore. All animal trials were executed according to local and worldwide procedures followed by the Wet op de dierproeven (article 9) of Dutch law (international) and an associated rule planned via the Bureau of Animal Research Licensing, Local University as detailed in our earlier papers (Ali et al., 2020; Hussain et al., 2020; Ara et al., 2020; Ali et al., 2020; Khan et al., 2019; Ali et al., 2019; Mumtaz et al., 2019; Mughal et al., 2019; Dar et al., 2019). The rearing and use of animal were carried out using NIH Publication "Guide for the Care and Use of Laboratory Animals" (NRC, 2011) and by the local bioethical committee of the University on animal experimentation.

2.2. Materials and chemicals

Raw silk cocoons were compassionately purchased from the Sericulture sector, the Department of Forest, and the Government of Punjab Ravi Road, Lahore. Silver nitrate ($AgNO_3$) (AR, 99.99 %) was acquired from Aladdin Corporation (Shanghai, China). Nolvadex (Tamoxifen Citrate) tablets, a non-steroidal anti-estrogen, were purchased from Ali Imran Pharmacy, Lahore. Each tablet was containing 45.6 mg of tamoxifen citrate which is equivalent to 30 mg of tamoxifen.

2.3. Extraction of sericin from raw silk cocoons

In the medical toxicology laboratory, Government College University Lahore, silk cocoons were cut into little portions to eradicate the larvae and autoclaved for 60 min at 120 °C by putting them into deionized water (Cho et al., 2003; Lamboni et al., 2015). Thereafter, fibroin was separated from the sericin solution with the help of a 12 kDa dialysis membrane (Pierce, USA), and silk sericin was used as a stock solution. From 1 g of raw silk cocoons, 10–20 mg silk sericin was achieved up and concentrated up to the required percentage.

2.4. Preparation of sericin powder and synthesis of sericin-$AgNO_3$ NPs

The obtained sericin solution was frozen and freeze-dried using a Hero LL 3000 lyophilizer under −20 °C to become sericin powder. A 1 % sericin stock solution was prepared by dissolving 1 g of sericin powder into 100 ml of doubled distilled water. 1 mM of silver nitrate ($AgNO_3$) solution was prepared and added dropwise into a 1 % solution of sericin. The mixture solution color changed into yellow–brown and placed into the sunlight for 36 h, an indication of sericin-$AgNO_3$ NPs composite. By using a 1 M solution of sodium hydroxide (NaOH), the pH of the solutions was adjusted from 9 to 11.

2.5. Characterization of sericin-$AgNO_3$ NPs

For the conformation of sericin-$AgNO_3$ NPs formation, different characterization techniques were used. Ultraviolet–visible spectroscopy (UV-1700, Shimadzu) was used to study the diagnostic peaks of sericin and sericin-$AgNO_3$ NPs with silver in the Nanotechnology Laboratory, Department of Chemistry, Government College University, Lahore. The morphological characters of NPs were pictured by using scanning electron microscopy (FEI NOVA 450 NanoSEM) and the elemental composition and concentration of nanoparticles were studied by using energy-dispersive X-ray (EDX) spectroscopy. Furthermore, Fourier-transform infrared (Bruker Alpha Platinum ATR, FTIR) was used to assess the chemical formation of sericin NPs at room temperature with a spectral range from 1000 to 4500 cm^{-1} available at Lahore University of Management Sciences (LUMS). An X-ray diffractometer (Rigaku Ultima IV) was used to examine the crystalline structure of sericin-$AgNO_3$ NPs. The samples were scanned in the 2θ range of 10°-80° with a scanning speed and step size of 3° min^{-1} and 0.02° respectively.

2.6. Cell culture and treatment of sericin and sericin-$AgNO_3$ NPs

Two selected breast cancer cell lines including MCF-7 and MDA-MB-231 were obtained from the University of Health Sciences Lahore. The cells were maintained and propagated in 90 % Roswell Park Memorial Institute (RPMI-1640) media supplement with 1 % streptomycin/penicillin and 10 % of fetal bovine serum (FBS). Cells were cultivated as adherent monolayers to just about 70– 80 %

confluence and sustained at standard culture conditions 37 °C in a humid atmosphere of 5 % CO_2.

2.7. In vitro cytotoxicity of sericin and sericin-$AgNO_3$ NPs / cell proliferation assay

Cells were treated with the selected compound and its NPs fractions followed by calculation of the cell viability via MTT (3-{4, 5-dimethylthiazol- 2- yl}-2, 5- diphenyl tetrazolium bromide) dye reduction solution. The cells were counted by Neubauer's chamber, placed in RPMI-1640 complete media, and seeded in two 96-well plates of MDA-MB-231 and MCF-7 cell lines at a given concentration of pre-optimized cell density (4×10^3 cells/100 µL medium/well) and incubated for 24 h at 37 °C. After 24 h cultures, the cells were exposed to different concentrations of sericin and sericin-$AgNO_3$ NPs (1 mg/mL, 0.5 mg/mL, 0.1 mg/mL) dosage, $AgNo_3$-NPs having a volume equal to sericin-$AgNO_3$ NPs for cytotoxicity comparisons and tamoxifen (10 µg/mL, 5 µg/mL, 2 µg/mL, 1 µg/mL) as a standard drug. After treatment, the cells culture plates were incubated for another different period including 24 h, 48 h, and 72 h respectively (Lv et al., 2018).

As a cytotoxicity test compound, the media contained sericin and sericin-$AgNO_3$ NPs (5 mg/mL stock solution) in different volumes of 20, 10, and 2.5 µL/well. As a positive control, 1 mg/mL of tamoxifen was added in different volumes of 1.2, 0.6, 0.24, and 0.12 µL/well. AgNPs were used with an equal volume of sericin-$AgNO_3$ NPs for association and to test out the antiproliferative activities/cytotoxicity of the sericin-$AgNO_3$ NPs themselves. After removal of the solution, 20 µL/well of MTT dye (5 mg/mL in media, Sigma, USA) was added to each well of the 96-well plate. After 4 h incubation, MTT solution was gently removed by micropipette, and added dimethyl sulphoxide (DMSO) (Sigma, USA) solution (50 µL/well) in each well. Viable cells were calculated by using an ELISA plate reader (Anthos Mikrosysteme, Krefeld, Germany) at 545 nm absorbance (with a reference filter of 620 nm). Measurements were achieved 3 times, and the percent survival of cell viability was calculated graphically by GraphPad Prism software. Every experiment was performed three times (Mandal and Kundu, 2009).

2.8. Expression modification by RT-PCR analysis

Both selected cell lines were seeded in 6-well plates at different concentrations of cells/well and given incubation for 24 h. The media of cells were removed, and the different concentrations of selected compounds including AgNPs, Sericin, sericin-$AgNO_3$ NPs, and Tamoxifen as over mention intermingled with cells. After 72 h of action, RNA extraction was performed from the cell pallet with a commercially available kit (Thermo Fisher Scientific, Cat#K0731, Germany). Complementary DNA (cDNA) was isolated from RNA samples with Maxima reverse transcriptase (Thermo Fisher Scientific, Cat#K1622, Germany) on ice, due to the kit manufacturer's process by way of oligo dT primer at different temperature conditions for different periods such as 42 °C in favor of 60 min, 70 °C used for 5 min, and 4 °C in favor of hold. Gene expression studies of selected genes were performed using 1 µg of cDNA along with gene specific primers, SybrGreen master-mix and Quantstudio 3 real-time PCR system. The reaction conditions of RT-PCR were as followed: degeneration at 95 °C for 5 min, 40 cycles of denaturation at 95 °C intended for 20 *sec*, renaturation for 30 s at 59 °C, and extension for 40 s at 72 °C. The primers were synthesized by using Primer 3 software, melting temperature (™) was calculated by Oligocalc software, and the qRT-PCR primer sequences were listed in Supplementary Table 1. With the help of the 2-ΔΔCT formula (Livak and Schmittgen, 2001), the fold changes in RNA expression levels were calculated. The hypoxanthine phosphoribosyl transferase 1 (HPRT1) gene was used as a reference gene for the normalization of the data set and each sample was repeated in triplicate.

2.9. Nuclear DNA staining

The apoptotic effects of sericin, sericin-$AgNO_3$ NPs, and Tamoxifen against MCF-7 and MDA-MB-231 cells were investigated by fluorescent nuclear dye using 4, 6-diamidino-2-phenylindole, dihydrochloride (DAPI) in comparison with untreated control cells. In a 6-well cell plate, the cells of both selected cell lines were seeded and treated with different concentrations of sericin (0.5–1.0 mg/mL), sericin-$AgNO_3$ NPs (0.5–1.0 mg/mL), Tamoxifen (2 µg/mL, 5 µg/mL, 10 µg/mL), along with a comparison with individual silver nanoparticles volume equal to sericin-$AgNO_3$ NPs and placed for 72 h. After the treatment with tested compounds, the cells were rinsed 3 times through PBS and fixed at room temperature using 4 % formaldehyde for 10 min. After permeabilization through 0.2 % Triton X-100, the cells were stained through DAPI dye for 2 min at a dosage of 0.5 µg/mL. After removing the DAPI dye, the cells were rinsed 3 times using a phosphate buffer solution and imaged using a phase-contrast fluorescent microscopy (EVO fluorescence microscope, Thermo Fisher Scientific, Germany). Every cell has glowing nuclear fragmentation and condensed nuclei were used as apoptotic cells. The untreated control cells were used as a negative control and the tested compound cells were used as treatment cells (El-Fakharany et al., 2020).

2.10. Data Analysis/Statistical analysis

For statistical analysis of data and appropriate statistical tests, GraphPad Prism 9.0 was applied accordingly. All the data were presented as a one-way analysis of variance (ANOVA), and mean ± standard deviation (SD), while statistically significant values showed by *P values* ($P < 0.05$).

3. Results

3.1. UV visible spectrum analysis

After ultra-visible (UV–vis) analysis, the spectrometer gave absorption peaks of individual sericin at the wavelength range of 216 to 274 nm instead of sericin-$AgNO_3$ NPs giving absorption peaks at the wavelength of 416–426 nm (Supplementary Fig. 1) showing the formation of silver nanoparticles (Muhammad Tahir et al., 2020).

3.2. Morphology and elemental analysis of sericin-$AgNO_3$ NPs through SEM and EDX

The image of SEM showed that the majority of sericin-$AgNO_3$ NPs were spherical, but some had hexagonal and triangular formations with a size range of 57 nm (Supplementary Fig. 2), while characteristics peaks produced by EDX recommended the presence of silver accompanied by some other elements such as carbon, calcium, oxygen, potassium, Aluminum, nitrogen and some other elements (Supplementary Fig. 3) (Muhammad Tahir et al., 2020).

3.3. FT-IR spectra analysis

Sericin showed the spectral bands at 1062 cm^{-1}, 1234 cm^{-1}, 1392 cm^{-1}, 1593 cm^{-1}, 2985 cm^{-1} and 3271 cm^{-1}. Whereas conjugation of silver with sericin shifting the intensity of bands at 3275 cm^{-1} indicates the (NH—OH bond) stretching, 2987 cm^{-1} indicates the C—H bond, 1597 cm^{-1} shows the relation of Ag with OH group of sericin (C═O stretching), 1234–1397 cm^{-1} indication

of C—N stretching, and 1062 cm^{-1} represented the (Ag—O) peaks (Supplementary Fig. 4). The results indicated that the formation of sericin-$AgNO_3$ NPs did not change the structure of individual sericin molecules.

3.4. XRD measurement

The XRD pattern of diffraction showed that sericin-$AgNO_3$ NPs face-centered cubic crystalline structure due to the reduction of Ag^+ to metallic Ag^0. The characteristics of diffraction peaks at scattering angles (2θ) of about 38.2°, 45.1°, 64.4°, and 78.7° which are attributed to (111), (200), (220), and (311) planes of the silver, respectively as shown in (Fig. 1).

3.5. Cytotoxicity effects of sericin and its nanoparticles against MDA-MB-231 and MCF-7 cells

Both selected cancer cell lines were treated through ever-increasing doses of AgNPs, sericin, sericin-$AgNO_3$ NPs (0.1–1.0 mg/mL), and standard drug tamoxifen (1, 2, 5, 10 μg/mL). Sericin and sericin-$AgNO_3$ NPs stimulate considerable time and dose-dependent antiproliferative properties in both types of cells. After 24 and 48 h treatment, MCF-7 cell lines were about less sensitive to sericin and sericin-$AgNO_3$ NPs at the highest dose (1 mg/mL) as shown in Fig. 2D and E, while after 72 h treatment cells were more sensitive to sericin and sericin-$AgNO_3$ NPs (41 %) as shown in Fig. 2F. A similar pattern of results was also calculated in the case of MDA-MB-231 cells for both tested compounds and all given time intervals but the cell inhibition rate (20 %) was less (Fig. 2A, B, C) than compared to MCF-7 cells. From the above-mentioned results, we declared that both sericin and sericin-$AgNO_3$ NPs showed significant inhibition of growth after a time interval as well as dose-dependent manners. The best possible concentrations, following the need for a further experimental procedure, were chosen depending on this preliminary viability process and applied in all other further considerations of this research.

3.6. RT-PCR analysis

To have further confirmation of Sericin and sericin-$AgNO_3$ NPs capability to induce apoptotic properties including fragmentation of DNA nuclei and shrinkage of cells, we performed the expressional profiles by qRT-PCR methodology. For this purpose, cells were grown in cell culture media and treated with different doses of $AgNO_3$, Sericin, sericin-$AgNO_3$ NPs (0.5, 1 mg/mL), and Tamoxifen (2, 5, 10 μg/mL). The molecular strategy confirmed the stimulation of growth arrest and cyclin-dependent kinase inhibitors (CDKN1A, CDKN1B) and DNA damage (GADD) family genes in human breast tumor cells. In the case of the MDA-MB-231 cells, the CDKN1A, and CDKN1B showed maximum induction by 4.5- and 2.5-fold, while GADD family-like GADD34, 153, A, B, and G showed maximum induction by 2.8-, 7.2-, 4.5-, 2.6-, and 34.3-fold as mention in (Fig. 3). For the MCF-7 cells, the maximum induction for CDKN1A, and CDKN1B followed the same pattern by 4.1-, 3.1-fold, where the for GADD34, 153, A, B, G, and 153 maximum induction were 7-, 19.8-, 3.1-, 5.7-, and 7.8-fold (Fig. 4).

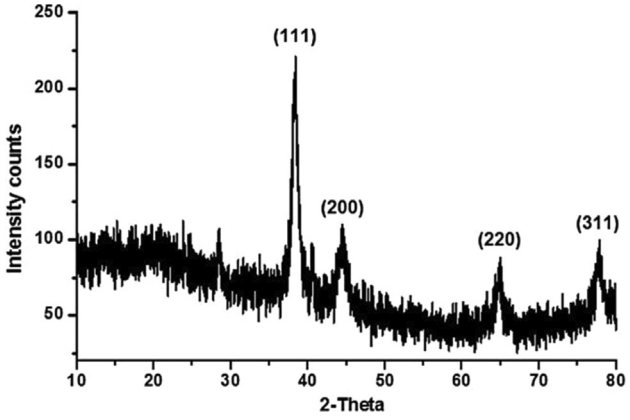

Fig. 1. X-ray Diffraction analysis.

3.7. Nuclear DNA condensation/fragmentation

The ability of sericin and sericin-$AgNO_3$ NPs to induce nuclear and DNA condensation in the chosen human breast cancer cell lines like MDA-MB-231 and MCF-7 cells were studied for the determination of either apoptotic cell death concerning cell cycle arrest or taking part in the given cytotoxic inhibition. The cells were treated with different dosages of sericin, and sericin-$AgNO_3$ NPs were used for 72 h and examined by fluorescence microscopy which guided to apparent disruptive alterations in the nuclei of the cells. The usage of various doses of tested compounds revealed the morphological alternations of apoptotic cell death such as chromatin condensation, nuclear fragmentation, membrane blabbing, nuclear shrinkage, and formation of apoptotic bodies. At lower concentrations, chromatin condensation was seen, whereas the effects were further significant at higher doses of test compounds in both selected human breast cancer cells such as condensation and nuclear shrinkage. Fig. 5 shows the cells of MDA-MB-231 with minor DAPI positively stained cells, although the most significant results of sericin and sericin-$AgNO_3$ NPs were shown at the highest dose 1 mg/mL. Meanwhile, Fig. 6 shows the comparison of untreated control and treatment cells of the MCF-7 cell line with various doses of above mention compounds for 72 h cells. After treatment with selected doses of sericin and sericin-$AgNO_3$ NPs, the cells have changed into a round shape and lost their original spindle shape concerning dose-dependent manners. Results indicated that nuclei become more intensely glowing with ever-increasing doses of sericin, and sericin-$AgNO_3$ NPs (1 mg/mL) as well as their chromatin fragmentation and condensation.

4. Discussion

In recent years, the usage of natural agents for the treatment of cancer has been one of the most crucial fields of study for cancer prevention. For the identification of chemoprevention and treatment of cancer one of the best key objectives is the utilization of natural compounds with minimum side effects to induce apoptosis in cancerous cells (Chon et al., 2013). Silk sericin produced by the silkworm gland has shown enormous perspective as a therapeutic material as a result of different properties including, excellent reactivity, biodegradability, biocompatibility, and hydrophilicity. It's usually used in regenerative medicines as a copolymer with side-chain polymers to form a variety of scaffolds in the field of biomedicine (He et al., 2017). Nanotechnology and nanomedicine have played a potential role in pharmaceutical and drug delivery approaches like anti-viral, anti-cancer, anti-fungal, and anti-microbial. Several manuscripts reported that AgNPs act as anti-bacterial as well as anti-fungal properties. However, the release of silver ions from these NPs causes mitochondrial dysfunction and induction of ROS that cause chromosomal alternations and DNA damage (Lv et al., 2018). To overcome the problem of cytotoxicity, in this current study we worked on sericin protein for the disperser and as a surface modifier in silver NPs production to get ready novel sericin-$AgNO_3$ NPs and talk about their biological

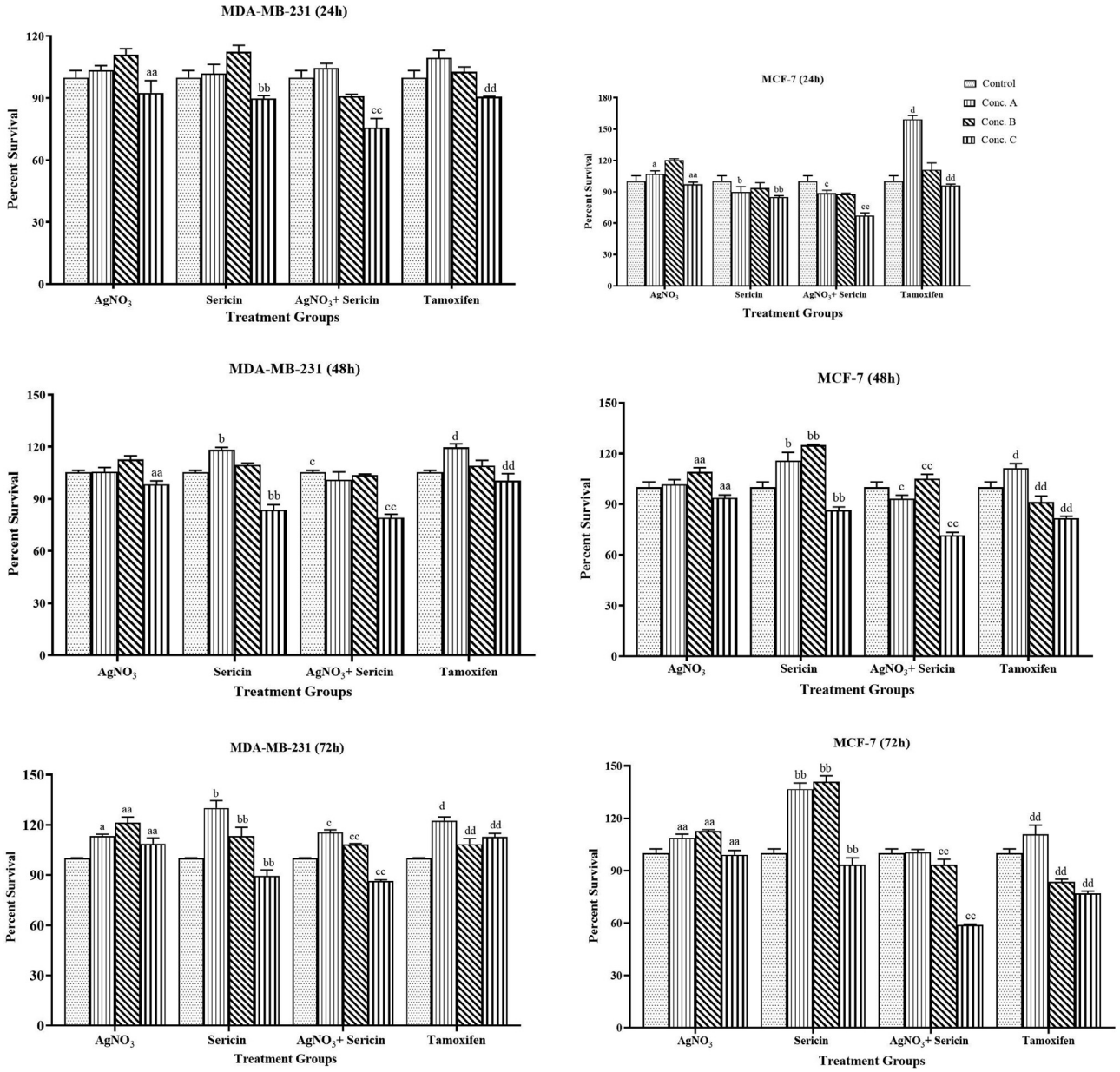

Fig. 2. Anti-proliferative effects of $AgNO_3$, Sericin, Sericin-$AgNO_3$ NPs, and standard drug Tamoxifen after 24, 48, and 72 h treatment in both selected cancerous cell lines. Antiproliferative effects in selected cells including MDA-MB-231 (A, B, C) and MCF-7 (D, E, F) were calculated through an MTT dye reduction assay. An alphabet represents significant cytotoxic effects ($P < 0.05$) on cells. "a" showed a significant difference between control and Conc. A, B, and C of $AgNO_3$ (0.1, 0.5, 1 mg/mL), "b" showed a significant difference between control and Conc. A, B, and C of Sericin (0.1, 0.5, 1 mg/mL), "c" showed a significant difference between control and Conc. A, B, and C of Sericin-$AgNO_3$ NPs (0.1, 0.5, 1 mg/mL), and "d" showed significant differences between control and Conc. A, B, and C of Tamoxifen (1, 2, 5, 10 μg/mL).

properties along with subsequent molecular alternations in two breast cancer cell lines.

The formation of sericin-$AgNO_3$ NPs was confirmed by different characterization techniques such as UV–vis spectral analysis, SEM, EDX, and FTIR. The UV–vis analysis showed the absorption peaks at 416 nm which indicated the formation of sericin-conjugated $AgNO_3$ NPs. In a previous study, similar outcomes have reported the spectrum of silver-conjugated NPs ranged from 412 to 425 nm (Al Masud et al., 2021). SEM images revealed that the majority of sericin-$AgNO_3$ NPs were spherical, but some had hexagonal and triangular shapes which are similar to the previous studies (Shah et al., 2019). Furthermore, EDX and FTIR analysis describe the elemental composition of NPs and are confirmed by some previous studies (Muhammad Tahir et al., 2020). FTIR spectra evolution showed the spectral bands of sericin at 1062 cm^{-1}, 1234 cm^{-1}, 1392 cm^{-1}, 1593 cm^{-1}, 2985 $cm^{-1,}$ and 3271 cm^{-1}, meanwhile, conjugation of silver with sericin shifting the intensity of bands to some extent at 3275 cm^{-1} indicates the (NH-OH bond) stretching, 2987 cm^{-1} indicate the C—H bond, 1597 cm^{-1} shown the relation of Ag with OH group of sericin (C═O stretching), 1234–1397 cm^{-1} indication of C—N stretching, and 1062 cm^{-1} represented the (Ag—O) peaks. Many other researchers revealed FTIR results of sericin-conjugated $AgNO_3$ NPs and also described the same FT-IR peaks as in our study, but some also showed slightly variable results (Dsugi and Elbashir, 2015). XRD measurement has shown that sericin-$AgNO_3$ NPs were crystalline in the structure having characteristics at scattering angles (2θ) of about 38.2°, 55.1°, 64.4°, and 78.7° which are attributed to (111), (200),

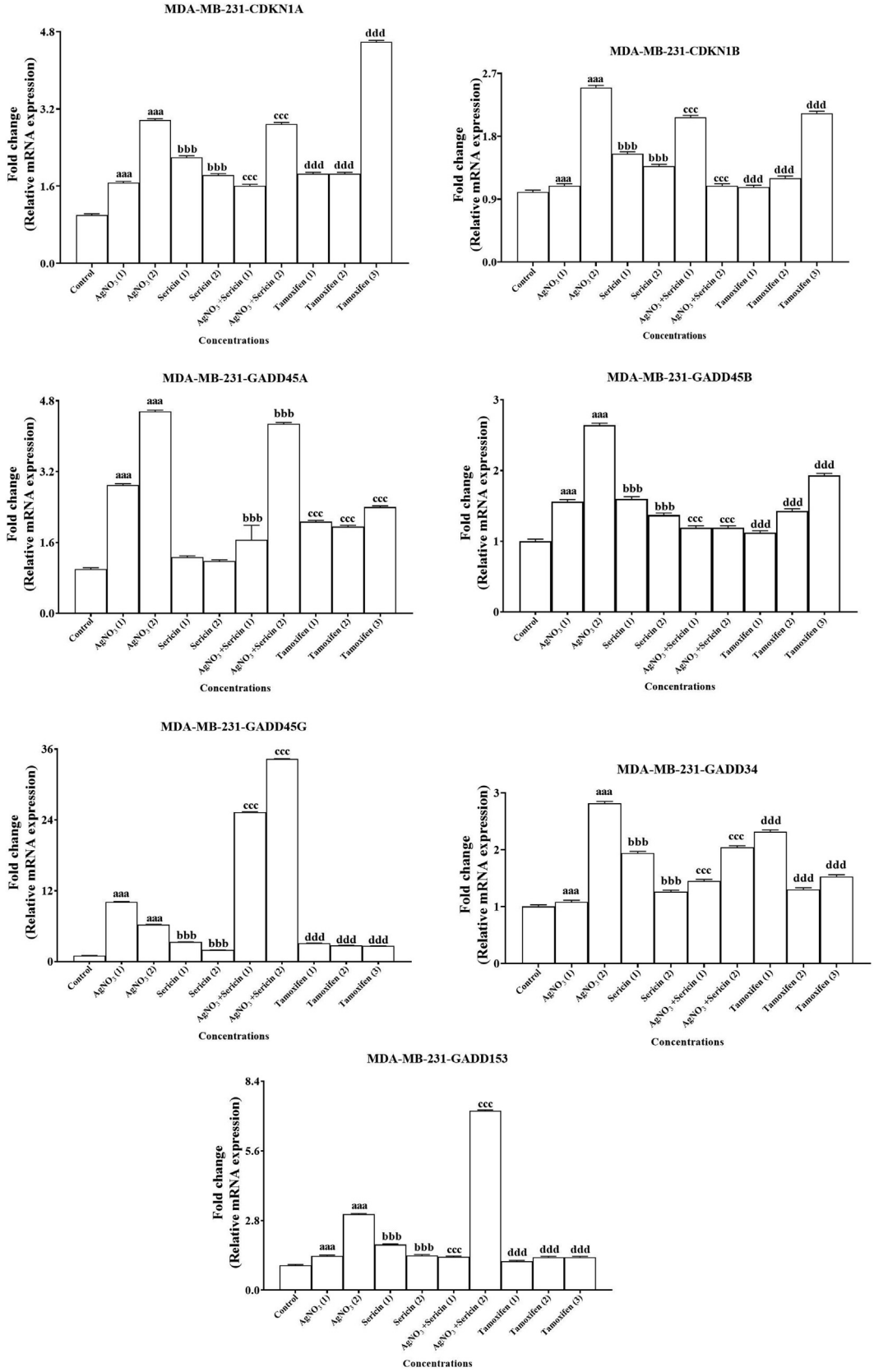

Fig. 3. qRT-PCR expression profiles of CDKN1A, CDKN1B, GADD 45A, B, G, 34, 153 of MDA-MB-231 cell line qRT-PCR expression profiles of cyclin-dependent kinase inhibitor (CDKN1A, CDKN1B), cell cycle relevant genes (GADD45A, B, G, 34, 153) of MDA-MB-231 cell line treated with various dosages of $AgNO_3$, Sericin, and Sericin-$AgNO_3$ NPs (1, 0.5 mg/mL), along with standard drug Tamoxifen (10, 5, 2 μg/mL) respectively. Fold change with relative mRNA expression was calculated by GraphPad Prism 8 software. An alphabet represents significant induction of cyclin-dependent kinase inhibitors (CDKN1A, CDKN1B) and GADD family genes ($P < 0.05$). "a" represented a significant difference among untreated control (U.C) and $AgNO_3$ (0.5, 1 mg/mL), "b" demonstrated significant difference among U.C and Sericin (0.5, 1 mg/mL), "c" represented significant difference among untreated control and Sericin-$AgNO_3$ NPs (0.5, 1 mg/mL), and "d" represented significant difference among U.C and Tamoxifen (2, 5, 10 μg/mL).

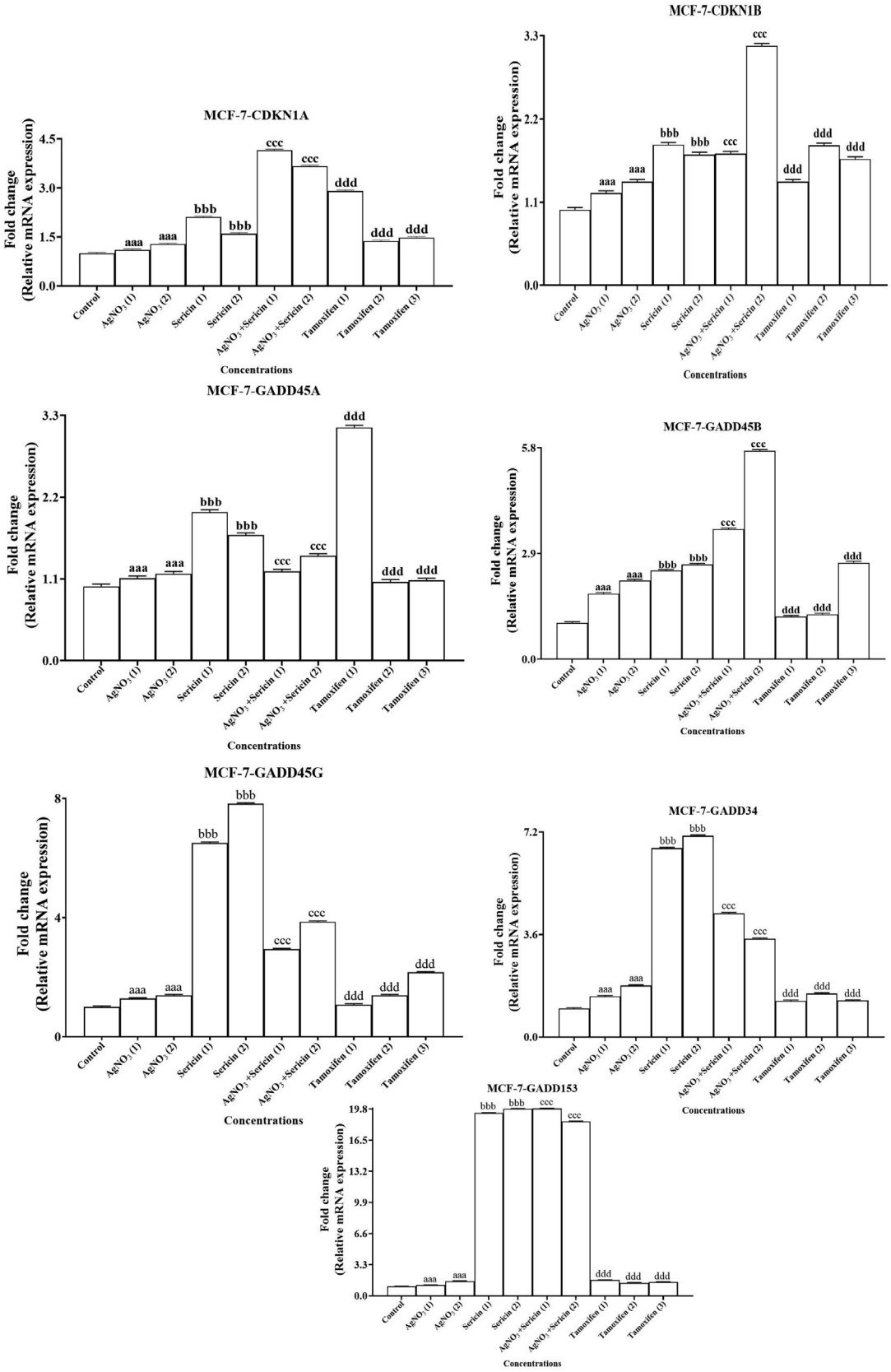

Fig. 4. Qrt-pcr expression profiles of cdkn1a, cdkn1b, gadd 45a, b, g, 34, 153 of mcf-7 cell line qRT-PCR expression profiles of cyclin-dependent kinase inhibitor (CDKN1A, CDKN1B), cell cycle relevant genes (GADD45A, B, G, 34, 153) of MCF-7 cell line, treated with various concentrations of $AgNO_3$, Sericin, Sericin-$AgNO_3$ NPs (0.5, 1 mg/mL), and standard drug Tamoxifen (2, 5, 10 μg/mL).). Fold change with relative mRNA expression was calculated by GraphPad Prism 8 software. An alphabet represents significant induction of cyclin-dependent kinase inhibitors (CDKN1A, CDKN1B) and GADD family genes ($P < 0.05$). "a" revealed significant difference among U.C and $AgNO_3$ (0.5, 1 mg/mL), "b" revealed significant difference among untreated control and Sericin (0.5, 1 mg/mL), "c" showed a significant difference between U.C and Sericin-$AgNO_3$ NPs (0.5, 1 mg/mL), and "d" represented the significant difference between U.C and Tamoxifen (2, 5, 10 μg/mL).

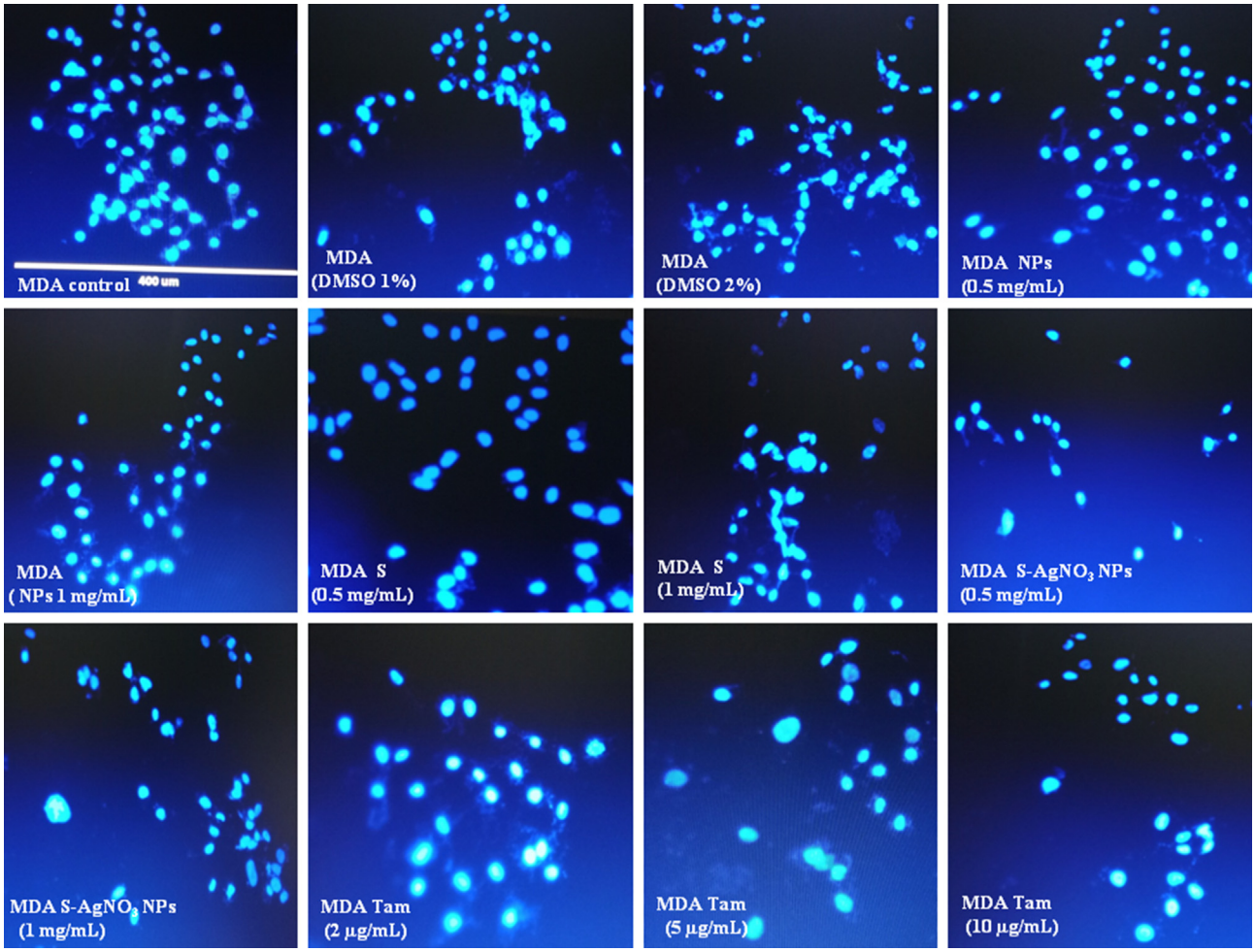

Fig. 5. Photomicrographs of MDA-MB-231 cells stained with DAPI dye, studied by fluorescent microscopy under a scale bar selected for all images are 400 µm. Cells were exposed through $AgNO_3$ NPs, sericin and sericin-$AgNO_3$ NPs (0.5, 1.0 mg/mL), and tamoxifen (2, 5, 10 µg/mL).

(220), and (311) planes of the silver. Previous studies have also affirmed that resultant particles are the face-centered cubic structure of metallic AgNPs.

In the second step, cytotoxicity levels of sericin and sericin-$AgNO_3$ NPs were analyzed in the selected human breast cancer cells with the help of the MTT dye reduction procedure. Sericin and sericin-$AgNO_3$ NPs demonstrated reasonable cytotoxic effects with low usage of concentrations with minimum side effects, but anti-proliferation levels vary among two cell lines (2 to 35-folds). MDA-MBA-231 cells were less sensitive as compared to the MCF-7 cells. For the MCF-7, a clear plateau for a high concentration of sericin and sericin-$AgNO_3$ NPs (1 mg/mL), while the sensitivity level of MDA-MB-231 cells showed a concentration-dependent, time, and balanced inhibition of sericin along with sericin-$AgNO_3$ NPs. In a previous study, bacterial silk sericin biopolymer (BNES) was used for human cancer cells treatment and the finding showed that BNES boosts the anti-tumor action with the help of inducing apoptosis and its mechanism of action is complicated due to different signaling pathways (El-Fakharany et al., 2020). Kaewkorn et al (2012), established that silk SER overcomes cytotoxicity by increasing apoptosis of colon tumor cells, consequently rising the action of caspase-3 along with a reduction in the expression of Bcl-2 (Kaewkorn et al., 2012). Moreover, the reason behind the antiproliferative outcomes of silk SER protein possibly will also attribute due to different pathways except for apoptosis including, arrest of the tumor cell cycle, suppression of angiogenesis, and inhibition of cancer development. Hastings and Kenealey (2017) worked on Avenanthramide-C, a novel phytochemical used to reduce cell viability against MDA-MB-231 cells during the apoptotic cell process. AVN-C, diminish the cell viability of MDA-MB-231 breast tumor cells using an apoptotic cell death pathway. They concluded that avenanthramide-C reduced cell viability, stain positive for caspase action and annexin V, as well as increased sub-G_1 population. All these activities indicated to Avenanthramide-C stimulate cell death in human breast tumor MDA-MB-231 cells and it can be used as a chemotherapeutic compound (Hastings and Kenealey, 2017). Similar results were yielded from our research study in which sericin and sericin-$AgNO_3$ NPs were used as novel therapeutic compounds against two human breast tumor cell lines such as MCF-7 and MDA-MB-231. The cell cytotoxicity action of both compounds revealed that they have reasonable cytotoxicity effects against both cell lines with low usage of concentrations. In another study, Vural. (2021) suggested that human serum albumin functionalized gold nanoparticles (HAS-Gold-NPs) were used to achieve tamoxifen delivery against two human breast tumor cells such as BT-474 and MDA-MB-231. The results indicated that the release pattern of tamoxifen entrapped by HAS-AuNPs stimulated cell death in concentration-dependent manners with the usage of various concentrations (1–100 µg/mL) (Akbal, 2021). Similar outcomes give up from our experimental study in which MCF-7 cells and MDA-MB-231 were treated through various dosages (0.1–1 mg/mL) of SER and sericin-$AgNO_3$ NPs and both

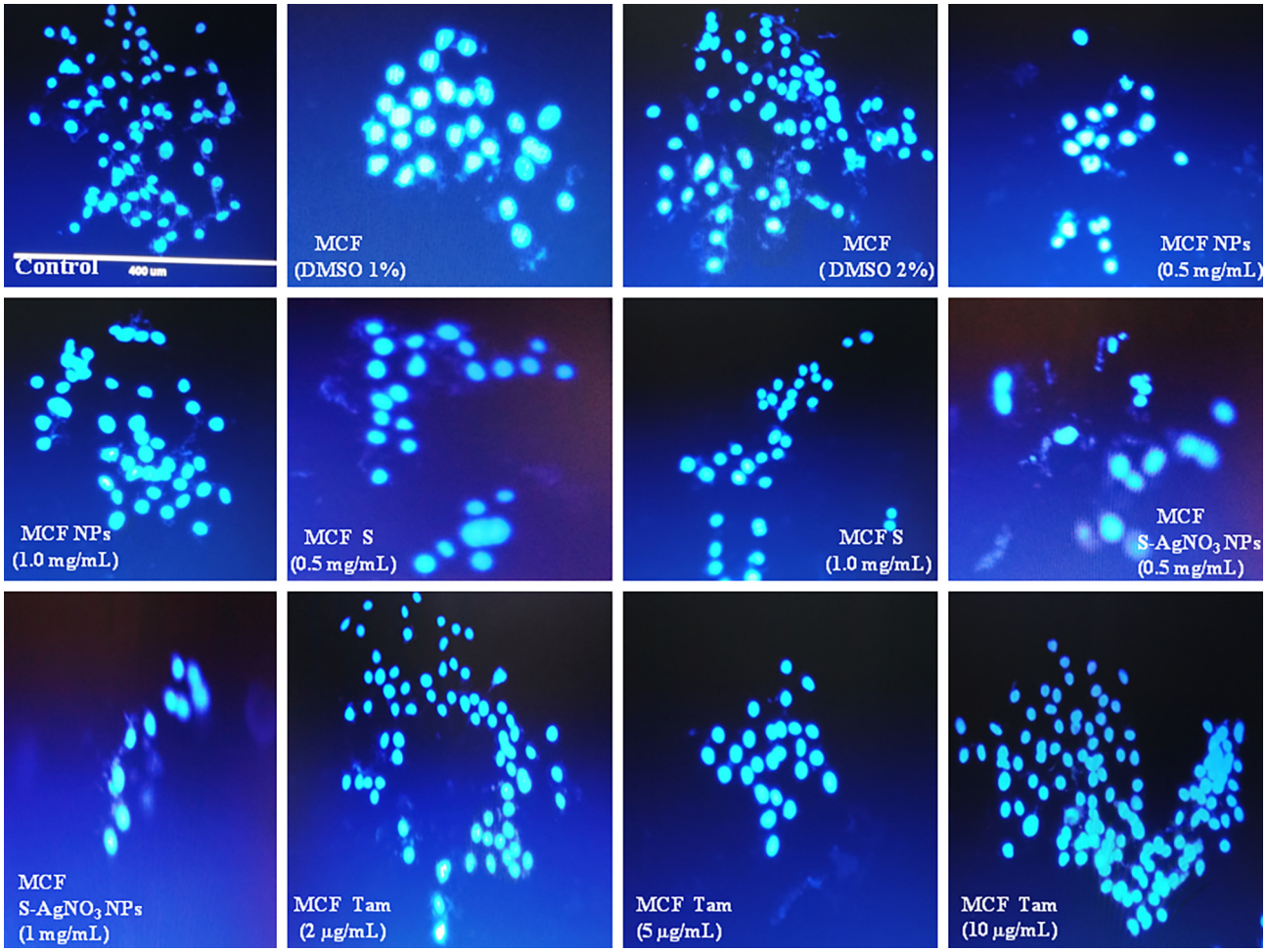

Fig. 6. Photomicrographs of MCF = 7 cells stained with DAPI dye, studied by fluorescent microscopy under a scale bar selected for all images is 400 µm. Cells were exposed through $AgNO_3$ NPs, sericin and sericin-$AgNO_3$ NPs (0.5, 1.0 mg/mL), and tamoxifen (2, 5, 10 µg/mL).

tested compounds also induced significant cell viability at 48 h and 72 h incubation (Fig. 2).

To move forward in approaching the probable mechanism displayed by sericin to induce anti-tumor and cytotoxic activity, an investigation of cell cycle delivery profiles was performed. For this reason, two human breast tumor cells were treated with various doses of sericin along with its nanoparticles (0.5, 1.0 mg/mL) for 72 h period in which maximum activity was calculated against both cell lines. Kumar and Mandal (2019) worked on silk sericin stimulating pro-oxidative stress which leads to apoptosis in cancer cells. The results declared that sericin contains polyphenols and flavonoid compounds that elevated ROS production in tumor cells. The elevated level of ROS caused cell cycle arrest at the cell cycle sub-G1 phase and resulted in apoptosis. Thus pro-oxidative stress induced by silk sericin suppresses cancer development demonstrating its prospective anti-tumor action (Kumar and Mandal, 2019). Similar results were shown in our study, as shown in Figs. 3 and 4, the silk sericin and sericin-$AgNO_3$ NPs can encourage cell cycle distribution confined in different main stages of the cell cycle such as G0, G1, G2, and M phases. The consequences showed that sericin and its nanoparticles as compared to untreated control cells, stimulated arrest in the sub-G1 and S-phase of treated cells and caused the apoptosis mechanism in a concentration-dependent approach. In a previous study, novel albumin-sericin NPs revealed a significant stimulation of apoptotic cell death and inhibition of cell development in the laryngeal cancer cells (Yalcin et al., 2019). Our outcomes are reliable to Yalcin et al. (2019) moreover as shown in Figs. 3 and 4, the sericin and sericin-$AgNO_3$ NPs caused the apoptosis mechanism in the main stages of the cell cycle in concentration-dependent manners. In a previous study, Riproximin a naturally occurring therapeutic agent used for the treatment of breast tumor cells like MDA-MB-231 and MCF-7. The outcomes showed that riproximin induced cytotoxic and apoptosis effects in both types of cells. Expression profiling indicated that significant induction of stress-related GADD family genes along with cytokines IL24/MDA-7, meanwhile prominent inhibition of BCL-family, genes-related migration such as RHO GTPase, and cell cyclin (Pervaiz et al., 2016). Similar results come from our study in which sericin along with sericin-$AgNO_3$ NPs was used for the treatment of both cancer cells, and RT-PCR results of the GADD family include GADD45A, B, G, 34, and 153 along with cyclin-dependent kinase inhibitors including CDKN1A, 1B showed pronounced significant induction 3.1 to 19.8-folds against MCF-7 cell line while induction against MDA-MB-231 cell line was 2.5- to 34.3-folds (Figs. 3, 4).

Additional authentication of the effective cell death action and anti-breast cancer activity of sericin and sericin-$AgNO_3$ NPs was established after 72 h treatment of both selected cell lines with the help of nuclear DNA staining with DAPI dye and capturing cellular morphological changes in these cells by phase-contrast fluorescent microscope. The dye can combine with different fragments of DNA, highlighting the cell death effect of SER and sericin-$AgNO_3$ NPs. Esamil et al. (2020) studied *in vitro* bacterial silk-like polymer, and bioactivities of SER protein and showed

results that indicated that bacterial sericin displayed satisfactory cytotoxic and cellular morphological alternations against MCF-7, A-549, Huh-7, and Caco-2 cancer cell lines (Esamil et al., 2020). Results revealed that nuclei of both human breast cancer cells turn into more brightly glowing with ever-increasing concentrations of SER and sericin-$AgNO_3$ NPs, along with condensation and chromatin fragmentation. Hence, sericin and sericin-$AgNO_3$ NPs showed anti-cancer activity against both selected human breast cancer cells. Asim et al. (2016) worked on riproximin, which has shown significant cytotoxic and apoptosis cell death effects. They declared that a significant nuclear fragmentation was seen in MDA-MB-231 and MCF-7 cell lines as causes for its apoptotic and cytotoxic effects and arrest in the S phase (Pervaiz et al., 2016). Similar results come from our research, we used a natural silk sericin protein along with sericin-$AgNO_3$ NPs nuclear shrinkage to stimulate DNA condensation in chosen tumor cells. Results indicated that nuclei become more intensely glowing with ever-increasing doses of sericin, and sericin-$AgNO_3$ NPs (1 mg/mL) as well as their chromatin fragmentation and condensation (Figs. 5, 6).

5. Conclusion

In vitro study revealed that sericin and sericin-$AgNO_3$ NPs showed anticancer action and showed cytotoxic effects against selected human breast cancer cells by stimulation of apoptosis and genetic alternations against cell cycle arrest genes. At the molecular level, sericin and sericin-$AgNO_3$ NPs support the stimulation of anticancer gene expression encouraging its tumor-specific cytotoxicity. Numerous anticancer effects of sericin and sericin-$AgNO_3$ NPs against selected breast tumor cell lines maintain their significant action as naturally presenting therapeutic compounds. However, further *in vivo* studies are needed for its use as a potent anticancer agent in pharmaceutical applications.

Declaration of Competing Interest

The authors declare that they have no known competing financial interests or personal relationships that could have appeared to influence the work reported in this paper.

Acknowledgment

The authors are grateful to the Department of Zoology, Government College University Lahore for providing facilities.

Funding

There was no funding for this study.

Availability of data and materials

Data will be available on request.

Author contributions

Samaira Mumtaz, Asim Pervaiz, and Shaukat Ali designed the study. Samaira Mumtaz Asim Pervaiz and Kinzah Kanwal executed the experimentations, Samaira Mumtaz, Asim Pervaiz, Shaukat Ali, and Muhammad Zahid Qureshi analyzed the data and prepared figures. Samaira Mumtaz, and Shaukat Ali, wrote the manuscript. All authors approved the manuscript.

Consent for publication

Not applicable.

Ethics approval and consent to participate

The research study was ethically approved with reference No. GCU-IIB-1064, from Government College University, Lahore. No human beings are involved in this study so consent to participation is not required.

Patient consent for publication

Not applicable.

Appendix A. Supplementary material

Supplementary data to this article can be found online at https://doi.org/10.1016/j.sjbs.2022.103551.

References

Akbal, V.O., 2021. Evaluation of protein functionalized gold nanoparticles to improve tamoxifen delivery: synthesis, characterization, and biocompatibility on breast cancer cells. Int. J. Polymeric Mat. Polymeric Biomater. 69 (4), 1–12.
Akram, M., Iqbal, M., Daniyal, M., Khan, A.U., 2017. Awareness and current knowledge of breast cancer. Bio. Res. 50 (1), 1–23.
Ali, S., Hussain, S., Khan, R., Mumtaz, S., Ashraf, N., Andleeb, S., Shakir, H.A., Tahir, H. M., Khan, M.K.A., Ulhaq, M., 2019. Renal toxicity of heavy metals (cadmium and mercury) and their amelioration with ascorbic acid in rabbits. Environ. Sci. Pollut. Res. Int. 26 (4), 3909–3920.
Ali, S., Awan, Z., Mumtaz, S., Shakir, H.A., Ahmad, F., Ulhaq, M., Tahir, H.M., Awan, M. S., Sharif, S., Irfan, M., Khan, M.A., 2020. Cardiac toxicity of heavy metals (cadmium and mercury) and pharmacological intervention by vitamin C in rabbits. Environ. Sci. Pollut. Res. 27 (23), 29266–29279.
Al-Masud., Shaikh, M., Alam, H., Karim, Minnatul, M.M., Islam, M.A., Khan, M.A., 2021. Green synthesis of silk sericin-embedded silver nanoparticles and their antibacterial application against multidrug-resistant pathogens. J. of Genetic Eng. and Biotec. 19 (1), 1–11.
Ara, C., Asmatullah, N.B., Ali, S., Batool, F., Shakir, H.A., Arshad, A., 2020. Abnormal steroidogenesis, oxidative stress, and reprotoxicity following prepubertal exposure to butylparaben in mice and protective efect of Curcuma longa. Environ. Sci. Pollut. Res. 28 (9), 1–11.
Bin-Jumah, M., Monera, A.A., Albasher, G., Alarifi, S., 2020. Effects of green silver nanoparticles on apoptosis and oxidative stress in normal and cancerous human hepatic cells in vitro. Int. J. Nanomedicine. 15, 1537.
Casais-Molina, M.L., Cab, C., Canto, G., Medina, J., Tapia, A., 2018. Carbon Nanomaterials for Breast Cancer Treatment. J. Nanomater. 13 (2), 1–9.
Cho, K.Y., Moon, J.Y., Lee, Y.W., Lee, K.G., Yeo, J.H., Kweon, H.Y., Kim, K.H., Cho, C.S., 2003. Preparation of self-assembled silk sericin nanoparticles. Int. J. Biol. Macromol. 32 (1–2), 36–42.
Chon, J.W., Jo, Y.Y., Lee, K.G., Lee, H.S., Yeo, J.H., Kweon, H., 2013. Effect of silk fibroin hydrolysate on the apoptosis of MCF-7 human breast cancer cells. Int. J. Indust. Entomol. 27 (2), 228–236.
Dar, K.K., Ali, S., Ejaz, M., Nasreen, S., Ashraf, N., Gillani, S.F., Shafi, N., Safeer, S., Khan, M.A., Andleeb, S., Mughal, T.A., 2019. In vivo induction of hepatocellular carcinoma by diethylnitrosoamine and pharmacological intervention in balb c mice using Bergenia ciliata extracts. Braz. J. Biol. 79 (4), 629–638.
Dsugi, N.F.A., Elbashir, A.A., 2015. Supramolecular interaction of Moxifloxacin and β-cyclodextrin spectroscopic characterization and analytical application. Spectrochim. Acta Part A: Mole. Biomol. Spectrosc. 137, 804–809.
El-Fakharany, E.M., Abu-Elreesh, G.M., Kamoun, E.A., Zaki, S., Abd-EL-Haleem, D.A., 2020. *In vitro* assessment of the bioactivities of sericin protein extracted from a bacterial silk-like biopolymer. RSC Adv. 10 (9), 5098–5107.
Esamil, M., El-Fakharany, G.M.A.E., Elbadawy, A., Kamoun, Abd-EL-Haleem, A.E., Szada., 2020. *In vitro* assessment of the bioactivities of sericin protein extracted from a bacterial silk-like biopolymer. RSC Adv. 10, 5098–5107.
Han, Y., Fan, S., Qin, T., 2018. Role of autophagy in breast cancer and breast cancer stem cells (Review). Int. J. Oncol. 52 (4), 1057–1070.
Hastings, J., Kenealey, J., 2017. Avenanthramide-C reduces the viability of MDA-MB-231 breast cancer cells through an apoptotic mechanism. Cancer Cell Int. 17, 1–12.
He, H., Tao, G., Wang, Y., Cai, R., Guo, P., Chen, L., Zuo, H., Zhao, P., Xia, Q., 2017. In situ green synthesis and characterization of sericin-silver nanoparticle composite with effective antibacterial activity and good biocompatibility. Materials Sci. & Eng. 80, 509–516.

Hu, D., Li, T., Xu, Z., Liu, D., Yang, M., Zhu, L., 2018. Self-stabilized silk sericin-based nanoparticles: In vivo biocompatibility and reduced doxorubicin-induced toxicity. Acta Biomater. 74, 385–396.
Hussain, S., Ali, S., Mumtaz, S., Shakir, H.A., Ahmad, F., Tahir, H.M., Ulhaq, M., Khan, M.A., Zahid, M.T., 2020. Dose and duration-dependent toxicological evaluation of lead acetate in chicks. Environ. Sci. Pollut. Res. 18, 1–6.
Joseph, B., Raj, S.J., 2012. Therapeutic applications and properties of silk proteins from Bombyx mori. Front. Life Sci. 6 (3–4), 55–60.
Kaewkorn, W., Limpeanchob, N., Tiyaboonchai, W., Pongcharoen, S., Sutheerawattananonda, M., 2012. Effects of silk sericin on the proliferation and apoptosis of colon cancer cells. Bio. Res. 45, 45–50.
Khan, R., Ali, S., Mumtaz, S., Andleeb, S., Ulhaq, M., Tahir, H.M., Khan, M.K.A., Khan, M.A., Shakir, H.A., 2019. Toxicological efects of toxic metals (cadmium and mercury) on blood and the thyroid gland and pharmacological intervention by vitamin C in rabbits. Environ. Sci. Poll. Res. 26 (16), 16727–16741.
Kumar, J.P., Mandal, B.B., 2019. Silk sericin-induced pro-oxidative stress leads to apoptosis in human cancer cells. Food Chem. Toxicol. 123, 275–287.
Lamboni, L., Gauthier, M., Yang, G., Wang, Q., 2015. Silk sericin: A versatile material for tissue engineering and drug delivery. Biotech. Advances. 33 (8), 1855–1867.
Livak, Kenneth J., Schmittgen, Thomas D., 2001. Analysis of relative gene expression data using real-time quantitative PCR and the 2− ΔΔCT method. Methods 25 (4), 402–408.
Lv, X., Wang, H., Su, A., Chu, Y., 2018. A novel approach for sericin-conjugated silver nanoparticle synthesis and their potential as microbicide candidates. J. Microbiol. Biotechnol. 28, 1367–1375.
Mandal, B.B., Kundu, S.C., 2009. Self-assembled silk sericin/poloxamer nanoparticles as nanocarriers of hydrophobic and hydrophilic drugs for targeted delivery. Nanotechnology 20 (35), 355101.
Mody, V.V., Nounou, M.I., Bikram, M., 2009. Novel nanomedicine-based MRI contrast agents for gynecological malignancies. Adv. Drug Deliv. Rev. 61 (10), 795–807.
Mughal, T.A., Saleem, M.Z., Ali, S., Anwar, K.K., Bashir, M.M., Babar, M., Khan, M.A., 2019. Evaluation of hepatotoxicity of carbon tetrachloride and pharmacological intervention by vitamin E in Balb c mice. Pak. J. Zool. 51 (2), 755–761.
Muhammad Tahir, H., Saleem, F., Ali, S., Ain, Q.U., Fazal, A., Summer, M., Mushtaq, R., Tariq Zahid, M., Liaqat, I., Murtaza, G., 2020. Synthesis of sericin-conjugated silver nanoparticles and their potential antimicrobial activity. J. Basic Microbiol. 60 (5), 458–467.
Mumtaz, S., Ali, S., Khan, R., Andleeb, S., Ulhaq, M., Khan, M.A., Shakir, H.A., 2019. The protective role of ascorbic acid in the hepatotoxicity of cadmium and mercury in rabbits. Environ. Sci. Pollut. Res. Int. 26 (14), 14087–14096.
National Research Council, (U.S). 2011. Committee for the update of the guide for the care and use of laboratory animals. In: Guide for the care and use of laboratory animals. 8th edition. National Academies Press (US), Washington (DC).
Pervaiz, A., Zepp, M., Adwan, H., Berger, M.R., 2016. Riproximin modulates multiple signaling cascades leading to cytostatic and apoptotic effects in human breast cancer cells. J. Cancer Res. Clin. Oncol. 142, 135–147.
Saha, J., Mondal, H.M.I., Sheikh, K.M.R., Habib, M.A., 2019. Extraction, Structural and Functional Properties of Silk Sericin Biopolymer from Bombyx mori Silk Cocoon Waste. J. Text. Sci. Eng. 9 (01), 1000390.
Shah, A., Buabeid, M.A., Arafa, E.S.A., Hussain, I., Li, L., Murtaza, G., 2019. The wound healing and antibacterial potential of triple-component nanocomposite (chitosan-silver-sericin) films loaded with moxifloxacin. Int. J. Pharm. 564, 22–38.
Yalcin, E., Kara, G., Celik, E., Pinarli, F.A., Saylam, G., Sucularli, C., Ozturk, S., Yilmaz, E., Bayir, O., Korkmaz, M.H., 2019. Preparation and characterization of novel albumin-sericin nanoparticles as siRNA delivery vehicle for laryngeal cancer treatment. Prep. Biochem. Biotechnol. 49, 659–670.